FEBS Letters 588 (2014) 3631–3638

journal homepage: www.FEBSLetters.org

Review

High-speed atomic force microscopy: Imaging and force spectroscopy

Frédéric Eghiaian, Felix Rico, Adai Colom, Ignacio Casuso, Simon Scheuring *

U1006 INSERM, Aix-Marseille Université, Parc Scientifique et Technologique de Luminy, 163 avenue de Luminy, 13009 Marseille, France

ARTICLE INFO

Article history:
Received 30 April 2014
Revised 5 June 2014
Accepted 6 June 2014
Available online 14 June 2014

Edited by Elias M. Puchner, Bo Huang, Hermann E. Gaub and Wilhelm Just

Keywords:
High-speed atomic force microscopy
High-speed force spectroscopy
Membrane protein
Membrane structure
Titin
Actin cortex

ABSTRACT

Atomic force microscopy (AFM) is the type of scanning probe microscopy that is probably best adapted for imaging biological samples in physiological conditions with submolecular lateral and vertical resolution. In addition, AFM is a method of choice to study the mechanical unfolding of proteins or for cellular force spectroscopy. In spite of 28 years of successful use in biological sciences, AFM is far from enjoying the same popularity as electron and fluorescence microscopy. The advent of high-speed atomic force microscopy (HS-AFM), about 10 years ago, has provided unprecedented insights into the dynamics of membrane proteins and molecular machines from the single-molecule to the cellular level. HS-AFM imaging at nanometer-resolution and sub-second frame rate may open novel research fields depicting dynamic events at the single bio-molecule level. As such, HS-AFM is complementary to other structural and cellular biology techniques, and hopefully will gain acceptance from researchers from various fields. In this review we describe some of the most recent reports of dynamic bio-molecular imaging by HS-AFM, as well as the advent of high-speed force spectroscopy (HS-FS) for single protein unfolding.
© 2014 Federation of European Biochemical Societies. Published by Elsevier B.V. All rights reserved.

1. Introduction

Atomic force microscopy (AFM) was invented in 1986 [1], and probably is the best-known offspring in the family of scanning probe microscopies, at least in biological sciences. AFM frequently draws comparisons with another revolutionary invention that predates it by at least 100 years, the gramophone: Indeed, in its primary operation mode (also known as 'contact mode'), AFM measures the topography of a surface by scanning it horizontally with a sharp tip placed at the extremity of a cantilever. Deflections of the cantilever arising from interactions of the tip with bumps and clefts of the surface are detected using the 'optical lever' system [2], in which a laser beam is reflected on the backside of the cantilever towards a segmented photodiode. Any angle change as a result of cantilever deflection results in a signal change on the photodiode: To preserve both the tip and sample integrity, the cantilever deflection (in other words the tip-sample interaction force) is maintained to a constant setpoint value. Cantilever deflection therefore translates into a vertical motion of the tip (or the sample) to restore the setpoint force using feedback control. When utilized on solid surfaces (for example graphite), AFM is able to resolve single atoms [3,4], for review see [5]. This astounding vertical and lateral resolution capability – still a hallmark of AFM to this day – is determined not only by the detection system, but first and foremost by the dimensions of the apex of the scanning tip and the ability of piezoelectric actuators to apply sub-nanometer displacements to the cantilever in response to small deviations of the detected signal from the setpoint. An important step of development, enabling biological AFM, was the development of a liquid cell in which cantilever, tip and sample are permanently immersed in buffer solution [6]. However, in the case of biological samples, softer than graphite by orders of magnitude, non-destructive imaging at nanometer-resolution in physiological conditions (i.e. in aqueous buffer, at ambient temperature and pressure) requires the ability to control forces $\leqslant$ 100 pN. With a high optical lever sensitivity, one is able to control normal forces applied by the cantilever down to about 50 pN in liquid, enabling contact mode imaging of biological samples. Thus, although lateral scanning forces impose a restriction on the sample type to be imaged in contact mode, it has yielded fascinating insights into the organization of proteins in biological membranes [7–13].

In addition, AFM has opened novel research avenues in 'force spectroscopy' mode, where the tip indents and retracts from a sample with controlled force and velocity. This mode of operation allowed mechanical properties of cells to be determined [14,15], and the study of receptor/ligand unbinding and protein unfolding at the single molecule level [16–19].

Abbreviations: HS-AFM, high-speed atomic force microscopy; HS-FS, high-speed force spectroscopy

* Corresponding author. Fax: +33 4 91828701.
E-mail address: simon.scheuring@inserm.fr (S. Scheuring).

http://dx.doi.org/10.1016/j.febslet.2014.06.028
0014-5793/© 2014 Federation of European Biochemical Societies. Published by Elsevier B.V. All rights reserved.

Concomitant to these achievements, the advent of 'intermittent contact mode' (also known as 'AC mode' or 'tapping mode') extended the capacities of bio-imaging by AFM. Operated in this mode, AFM can scan fragile and loosely attached biological samples by reducing the tip-sample interaction time and eliminating friction forces. In theory, an AFM cantilever may be considered as a harmonic oscillator that can be brought into resonance by acoustic excitation. In AC mode, the oscillation amplitude may be used as feedback parameter, as it decreases upon contact of the tip with the sample. If the amplitude of the cantilever in contact is the setpoint value, then normal and lateral scanning forces are largely decreased if the setpoint is close to the free amplitude (i.e. when the tip is out of contact). In such operational conditions the sample is contacted by the tip only very briefly, during about 10% of the time interval at the bottom of each oscillation cycle. With that in hand, AFM operators could image a variety of soft biomolecules in their physiological environment, label-free, at a topography resolution close to that of cryo-electron microscopy.

However, AFM was severely limited by its image acquisition rate in AC mode (also in contact mode, though this is slightly faster), at least an order of magnitude slower than most biological processes. In intermittent contact modes the cantilever oscillates at resonance and height detection is based on the oscillation amplitude measurement, as a consequence the operation speed is primarily limited by the resonance frequency of the cantilever. That limit is in turn dictated by the cantilever dimensions, following the relation (for rectangular cantilevers only):

$$f_0 = \frac{1}{2\pi}\sqrt{\frac{k}{m}}, \qquad \text{and} \qquad k = E \cdot t^3 \cdot w/4L^3$$

where k is the spring constant, m the mass of the cantilever, and t, w, and L, the thickness, width and length of the cantilever and E the Young's modulus of the cantilever material [20].

Most commercially available AFMs are built to accommodate 50–500 μm long cantilevers, and as a consequence bio-imaging at nanometric resolution is generally achieved within a timescale of one to several minutes, thereby limiting bio-AFM imaging to structural applications of stable samples. Fortunately, the speed limitations of AFM was possible to be overcome: With cantilevers of the smallest possible size, yet with soft enough spring constant, high resolution scanning of biological samples at video rate, termed high-speed atomic force microscopy (HS-AFM), in physiological conditions is now possible [21].

First efforts in this direction pushed the image acquisition rate to 1 Hz [22], but further developments to increase the feedback response speed, improve the piezo scanner speed and stability, miniaturize the cantilever and optimize the optical detection system were required in order to push the scan rate below 1 Hz [23–25]. More than 10 years of technical development were required to achieve this and perform high-speed scanning with fast feedback response (the bandwidth of feedback control now reaches 100 kHz), controlling displacements in horizontal and vertical directions with nanometer accuracy, and to engineer soft ($k \sim 100$ pN/nm) and small ($\sim 2 \times 6$ μm) cantilevers with ~1 MHz resonance frequency in liquid. Ultimately, video-speed AFM imaging of biomolecular dynamics of single molecules at nanometric resolution became reality [26]: This remarkable feat was illustrated by direct imaging of Myosin-V walking on actin filaments [27]. Importantly, whereas the displacement of a fluorescent spot is observed in optical microscopy, or noise changes in an optical trapping experiment, in dynamic HS-AFM the molecule itself is visualized while working and moving on its biological track, providing concomitant structural and dynamic data. Besides the visual power of those movies, the insights that they have provided into the mechanics of myosin-V is unmatched by any other biophysical method: Not only did the observation confirm the hand-over-hand walking mechanism of myosin-V, it did reveal that the power stroke of this motor is driven by intramolecular mechanical tension [28]. Another nice example of direct observation of processive enzymatic action was cellulose processing by the enzyme cellulase, showing that pre-processing of cellulose may increase its conversion efficiency by reducing the occurrence of crowding-induced enzymatic 'halts', with important implications in biofuel engineering [29]. HS-AFM also enabled direct imaging of single molecule diffusion on and in membranes [30–32], amyloid fibril assembly [33], and the rotary catalysis of ATPase [34]. In spite of those breakthroughs, in which HS-AFM provided novel insights into fundamental biological problems probably inaccessible to any other technique that does not analyze structure and dynamics concomitantly, the technique remains little known to many biologists, and has gained only little recognition outside of biophysics. This is on the one hand due to the fact that the technique is young and complex, and only experts are able to take full advantage of its capabilities. On the other hand, the technique is still lacking standards and established sample preparation procedures. Today still, each bio-sample to be studied represents a full novel project for which preparation and analysis conditions must be established from scratch. These are major obstacles for a more generalized use in biology. For other techniques, like electron microscopy, researchers have invested considerable efforts to overcome such bottlenecks. Clearly, while the novel capabilities that HS-AFM offers – concomitant nanometer resolution real-space information and dynamics – makes the technique unique and complementary to other structural biology techniques, in order for AFM to be more widely used and accepted, these bottlenecks must be overcome.

In this review, we will show that in the last couple of years HS-AFM has demonstrated its power for combined dynamic structural and functional analysis on biological systems of increasing complexity from purified membranes to live cells, with tremendous potential to enhance its present capabilities through further technological development and improved amenability. We hope that this short review will motivate researchers from various fields to contribute to the efforts undertaken to make HS-AFM a widely used tool in biological sciences.

2. Main text

2.1. HS-AFM imaging: from isolated membranes to cells

AFM being a surface imaging technique, its usefulness in the characterization of membrane proteins in flat lipid bilayers comes naturally. Fundamental processes in the biology of prokaryotes and eukaryotes start at the cell membrane: those encompass passive and active transport of molecules, generation of a transmembrane potential and energy, signal transduction cascades, to name a few.

Membrane proteins have been – and are still to some extent – the orphans of structural and molecular biology. It took 25 years from the first soluble protein (myoglobin) X-ray structure [35] to the first membrane protein (reaction center) atomic structure determination [36]. At the date this review is written, scientists dispose of 1454 membrane protein structures of 464 unique proteins [37], while a total of 99293 structures were deposited in the protein data bank (PDB, [38]). Hence the structural information on membrane proteins of ~1% of all structures is still in unfavorable relation to the ~25% of all genes coding for membrane proteins [39].

Beyond structural analysis, the lateral organization of membrane proteins in the cell membrane, as well as the diffusion properties of individual proteins and/or the formation/dissociation of protein clusters have been recognized of crucial importance and

to modulate membrane protein function. HS-AFM being able to perform scanning of regions with about 100 nm size at a frame rate in the order of 100 ms and nanometer lateral resolution, gives us the opportunity to observe the diffusion, association/dissociation behavior and conformational changes of label-free membrane proteins in biological membranes. Furthermore, the high-resolution capability and high signal-to-noise ratio of HS-AFM further allows the study of dynamic membrane protein conformational changes, in case that they are slow (Fig. 1).

Bacteriorhodopsin (bR) forms highly ordered 2D arrays in the purple membrane of *Halobacterium (H.) salinarum*. Advantage has been taken from this arrangement for early structural analysis using electron crystallography [40]. However, the molecular basis and the energetic terms of the interactions for this architecture remained unknown. HS-AFM imaging has been used to image bR association and dissociation at array borders [41] (Fig. 1a). The dynamics of single molecules could be visualized and classified as a function of the number of molecular interactions that the observed bR molecules incurred before dissociation. It was found that bR molecules with two binding partners associated for longer time periods to the array than proteins that had only one neighbor. Statistical assessment of the dissociation frequencies allowed the calculation of the strength of a single bR–bR interaction of $-1.5k_BT$ (0.9 kcal/mol), resulting in a stability of about 5.4 kcal/mol for the purple membrane arrays, in good agreement with ensemble measurements by calorimetry. From dynamic HS-AFM observations of the geometrical behavior of single dissociating and associating bR molecules, the importance of exposed aromatic residues (tryptophans 10 and 12) for the formation of the trigonal bR packing in purple membrane could directly be established.

Bacteriorhodopsin has been identified and functionally characterized in the early 70's as a light-driven proton pump [42]. Over the following 25 years, the entire photocycle of bacteriorhodopsin was functionally characterized [43] and high-resolution X-ray structures determined [44]. It appeared as a promising and challenging task to study the bacteriorhodopsin photocycle by HS-AFM, and – maybe surprisingly – the findings provided novel unexpected insights into the bacteriorhodopsin photocycle, so far unappreciated by other biophysical and structural approaches. Because the photocycle of native bacteriorhodopsin is very fast, in the microsecond time range, for HS-AFM analysis a mutant bacteriorhodopsin (D96N) has been chosen that is known to perform the photocycle in a native manner but in the second time range [45]. An optical path has been integrated into the HS-AFM that allowed stimulation of bacteriorhodopsin within the experimental chamber using light pulses of different intensity and wavelength. Following light flash activation of absorbable wavelength, the cytoplasmic E–F loop of individual bR molecules moved by ~0.7 nm outwards from the bR trimer center (Fig. 1b). In contrast, light flashes of wavelength that cannot be absorbed by bacteriorhodopsin-bound retinal did not induce conformational alterations. Importantly, bR monomers of adjacent trimers within the purple membrane lattice showed cooperativity, providing a long-awaited explanation for the formation of the stable and large 2D-arrays. Clearly the cooperativity between neighboring molecules could only be assessed using a single molecule resolving technique and would be overseen in ensemble measurements, highlighting the power and need for the analysis of structural dynamics of membrane proteins of HS-AFM. Furthermore, the observed amplitude of the conformational change of the E–F loop is much larger than what was expected from X-ray structures of the protein in different states of the photocycle. This discrepancy could be explained in favor of the HS-AFM analysis due to potential limitation of the degree of movement of the protein loops in 3D crystals.

Casuso et al. performed a study of a trimeric bacterial outer membrane pore named 'outer membrane protein F' (OmpF) in

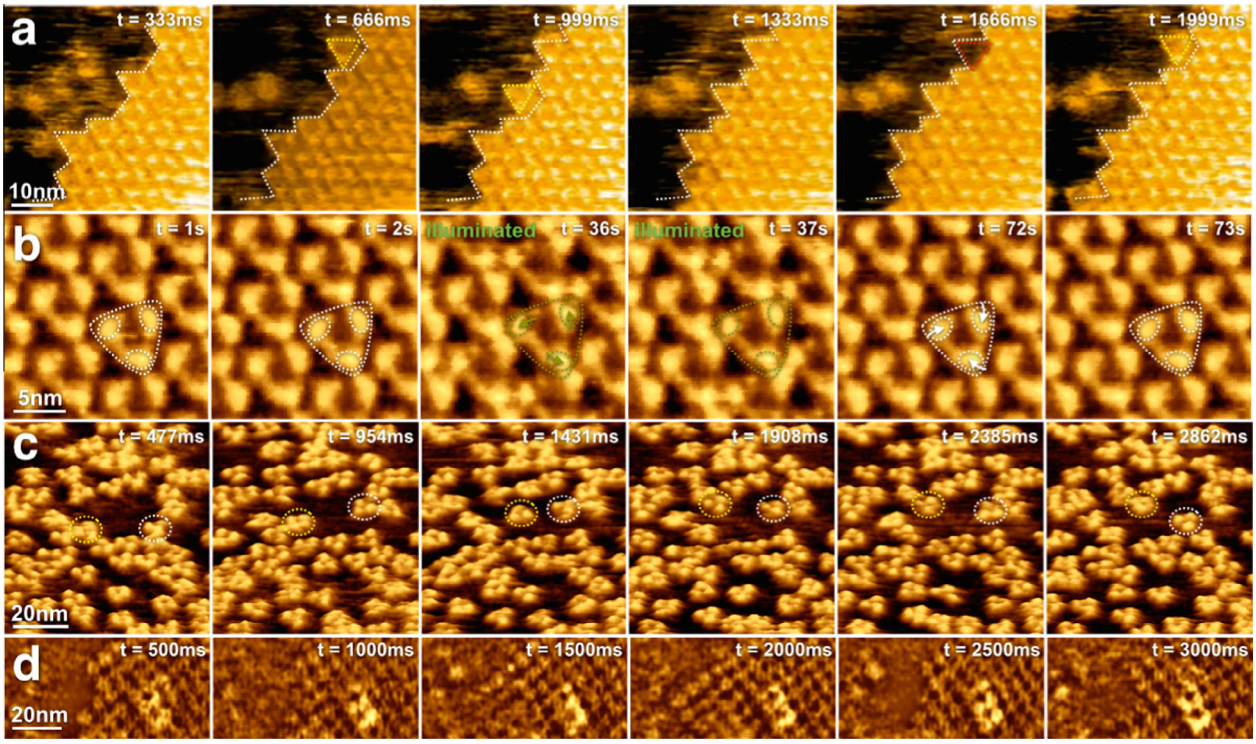

Fig. 1. HS-AFM imaging of native isolated or reconstituted membranes. (a) Association and dissociation dynamics of bR at purple membrane lattice edges, resulting in a -1.5 k_BT interaction energy between molecules. (b) Light-induced conformational changes of bR, revealing movement of the E–F loop with cooperativity of the monomers of adjacent trimers. (c) Lateral and rotational diffusion dynamics analysis of OmpF. Molecular motion scales inversely with the accessible free membrane space. (d) Association and dissociation dynamics of AQP0 at junctional microdomain edges in native eye lens membranes, resulting in a -2.7 k_BT interaction energy between molecules.

Escherichia coli lipid bilayers at protein densities mimicking that of the bacterial surface [31] (Fig. 1c). Molecule tracking of each individual protein in the membrane, defining localization and rotation angle, allowed the experiment-based calculation of an energy landscape of the interaction between membrane protein OmpF trimers within the membrane and mediated by the membrane. Furthermore the study showed that OmpF trimers tended to rotate in a defined trajectory during their approach and separation, allowing lipids to laterally intersperse the protein surfaces, and minimizing protein contact before they separated. OmpF evolved in a rich variety of local environments. Some molecules were able to diffuse freely in delimited areas while crowding of trimers led to encounters that resulted in stable assemblies and immobilization of proteins in the membrane. The distribution of OmpF in the membrane was analyzed revealing a fractal structure, which maximizes the membrane coverage of the protein, probably optimizing exposure of protein surfaces for the formation of complexes. The fractal coefficient found for OmpF distribution was characteristic of a process of diffusion-limited aggregation.

Similar to bacteriorhodopsin in *H. salinarum*, some membrane proteins form regular arrangements and gather in supramolecular domains in native mammalian membranes. In the membranes of fiber cells from the mammalian eye lens, lens-specific aquaporin-0 and connexons are the most abundant proteins. Conventional AFM allowed the characterization of the supramolecular arrangement of these proteins in junctional microdomains at high resolution showing the aquaporins assembly in regular square arrays edged and separated by densely but non-regularly packed connexons [46]. Both of these membrane proteins are not only channels, but act as cell adhesion molecules by means of their extracellular loops that interact homotypically with the proteins from the neighboring cell. HS-AFM provided novel insights into both the vertical (adhesion) and the lateral (in the membrane plane) associations of these junctional microdomain proteins [32]. The lens cell membrane preparations maintained the native double membrane architecture of the junctional microdomains. Using HS-AFM in contact mode applying additional forces, the junctional microdomains were dissected, revealing that the adhesion function of the proteins was cooperative, entire membrane patches dissociated at once. At high spatial and temporal resolution, HS-AFM could observe the assembly and disassembly of aquaporin-0 and connexons to and from junctional microdomains. Following the same statistical analysis of the image series as has been performed on bR [47], an interaction strength of $-2.7\ k_BT$ was determined for single aquaporin-0 interactions.

The studies of bR, OmpF and AQP0 likely reflect the dynamic behavior of membrane proteins in a native system, but the ultimate goal of biophysicists is to directly observe membrane proteins in their physiological environment in the living cell. Practically speaking, an AFM experiment is best performed on a flat, chemically homogeneous and well-controlled sample. In contrast, cells are extremely heterogeneous and complex objects from subcellular and molecular standpoints: Because AFM *per se* is "blind", using it to identify a region of interest to be scanned on the cell surface is difficult. Nowadays, commercially available AFMs may be mounted on inverted optical microscopes for cellular applications. However, combining optical microscopy with a HS-AFM setup is particularly challenging given the fact that its scanning elements were miniaturized to enhance scanning speed, and its design optimized for mechanical stability. There were two possibilities to achieve this goal: (i) Undertaking drastic modifications of the HS-AFM setup to make it mountable on an inverted optical microscope, keeping moving elements small, or alternatively, (ii) accommodate optical detection within the HS-AFM setup assuring its unchanged scanning performance. Recently this problem was addressed in two independent reports. Colom et al. present a hybrid HS-AFM/optical microscope that is based on the original HS-AFM design with the integration of an optical pathway [48], whereas Fukuda et al. re-designed a HS-AFM in "table-top" configuration for simultaneous HS-AFM/single molecule fluorescence imaging after mounting the HS-AFM on an inverted optical microscope [49] (Fig. 2).

In a typical high-speed AFM setup [23], a small mica disc (1.5 mm diameter) is glued to a 1.5 mm diameter glass rod of 2 mm height. This way, the mass added to the scanner is small (~9 mg) and the scanner resonance frequency in all directions is

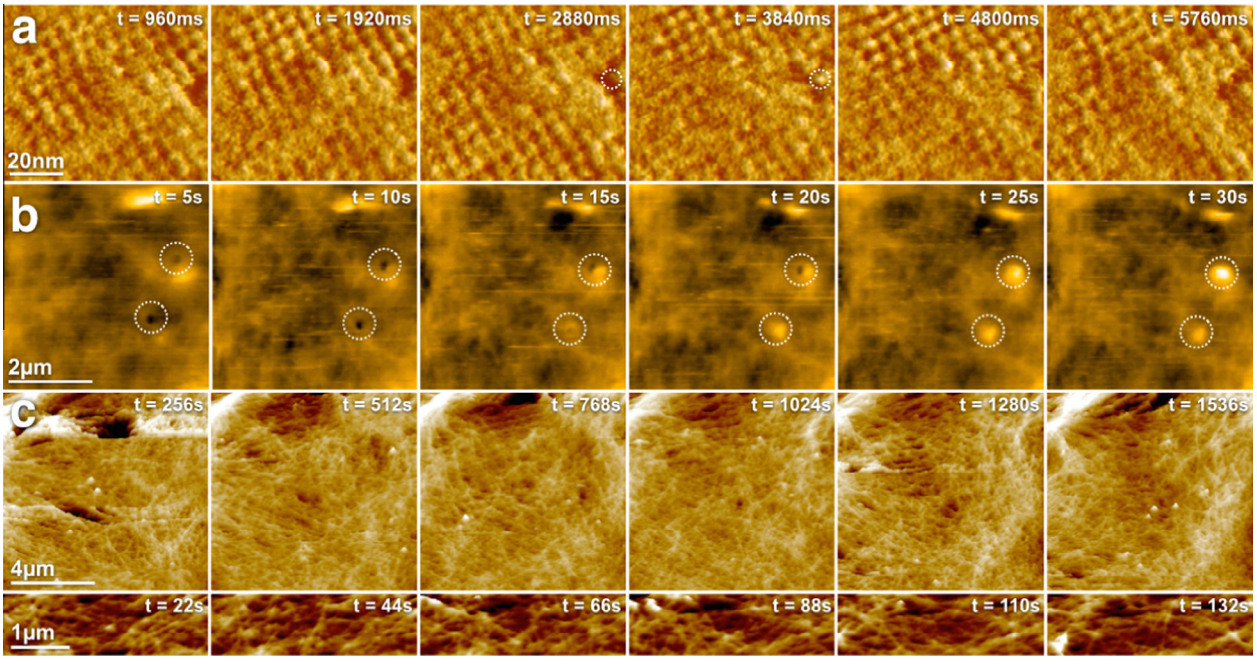

Fig. 2. HS-AFM applications on life cells. (a) High-resolution HS-AFM imaging of AQP0 in junctional microdomains in native eye lens cells. The dynamic association of individual AQP0 could be observed (outline). (b) Endocytosis events observed by HS-AFM on HeLa cells. (c) Dynamic PeakForce tapping imaging of the membrane cortex underneath the plasma membrane of 3T3 fibroblasts.

nearly unchanged. The strategy of Colom et al., was to substitute the glass rod by a small glass cube containing a mirror at a 45° angle with respect to the sample plane: The aim of this mirror cube was to inject bright-field illumination to the sample. The 20× objective that is part of the optical lever system was equally used in the optical microscope path, which was completed with an infinity tube lens and an objective for image formation on a CCD camera. The setup could also perform fluorescence imaging, as a fluorescent source was present in the back of the 20× objective. Potential interferences of the optical microscope, which works in visible light range with the optical lever detection system, which uses a near infra-red laser ($\lambda = 750$ nm) were precluded by the addition of a dichroic mirror with a 700 nm cutoff at the back of the objective, allowing reflection of the AFM near-infrared-laser to the split photodiode and transmission of the bright-field or fluorescent light. Using bright-field and fluorescence imaging a region of interest on a cell could be located and the tip be placed in this region with ~100 nm accuracy. GFP-expressing *E. coli* cells could be accurately detected and scanned by HS-AFM at a rate of 2.7 s per frame. Having validated the technique on bacteria, the lateral organization of aquaporin-0 (AQP0) within native sheep lens cells was investigated. The eye lens is a transparent tissue constituted of tightly packed fiber cells. AQP0 is a water channel that forms micro-domains involved in thin junctions between lens fiber cells. The integrity of those domains is crucial to the intercellular packing and to the transparence of the tissue: Cataract indeed arises from a disruption of AQP0 arrays. Fiber cells purified from sheep lens were used to study the AQP0 molecular architecture and dynamics at the plasma membrane using HS-AFM (see also Fig. 1d). Following tip placement on the cell, HS-AFM scanning was performed with a maximal acquisition time of 960 ms. Movies revealed the existence of mobile square AQP0 arrays at the surface of fiber cells (Fig. 2a): Analysis showed that the root mean square displacement of those arrays was proportional to the diffusion time, which demonstrated Brownian motion of AQP0 junctional microdomains. While the lens cell membrane is a highly specialized system, this study provided the first direct imaging of unlabeled membrane proteins diffusing at the surface of cells. The fact that AQP0 arrays are mobile may have relevance in the long-term maintenance of the functional integrity of the eye lens, particularly to withstand mechanical stress during accommodation, i.e. the shape change of the lens during focusing to different distances. Importantly, the above-described relatively simple modification of the HS-AFM turning it into a potent hybrid optical-HS-AFM, paved the way for many future nanometer-resolution imaging applications on live cells.

The strategy adopted by Fukuda et al. for implementation of simultaneous optical microscopy and HS-AFM was very different, as the authors drastically modified the design of HS-AFM to build a "table-top" configuration mountable on an inverted optical microscope. This configuration has the obvious advantage that all the most performing optical microscopy techniques, such as TIRF single-molecule imaging, could be performed simultaneously with HS-AFM [49]. In the "table-top" configuration the tip scans (in *X*, *Y* and *Z* directions) the sample surface. The hurdle of loss of laser positioning on the tip during *X*–*Y* scanning was overcome using a piezo-driven mirror tilter that continually re-adjusts the laser beam position on the cantilever. Although no cellular application was demonstrated in this report, Fukuda et al. proved that they can perform simultaneous single-molecule fluorescence and HS-AFM imaging of Myosin-V on actin, and the application of that setup to a variety of biological systems was therefore suggested [49].

Two other recent studies reported the use of HS-AFM scanning to imaging the dynamics at the plasma membrane of eukaryotic cell. First, Watanabe et al. developed a wide-range scanner [50], to enable long-range scanning of large samples at high-speed by magnifying the displacements of x and y piezoelectric elements using a leverage mechanism. As a result, the *X*–*Y* range of this scanner is 40 × 40 μm, whereas it was before limited to 1 × 4 μm. In addition the *Z*-range was extended to 2.5 μm *vs* 600 nm previously. With proper hysteresis compensation of the *X*–*Y* scan, a maximum rate of 2 s per frame was achieved on *Bacillus subtilis* bacteria. At this speed, excellent lateral and vertical resolutions were achieved as details of the cell wall and its destruction by lysozyme were seen. Furthermore imaging at 5 s per frame on HeLa cells directly showed significant biological events such as actin retrograde flow, and most importantly real-time single endocytosis events (Fig. 2b), demonstrating a lateral and temporal resolutions that goes beyond possibilities of optical microscopy on cells.

Second, in a recent report, Eghiaian et al. used a different AFM method to observe cellular dynamics at the plasma membrane level, but this time underneath it [51]. Taking advantage of a recently developed method named PeakForce tapping [52], imaging of the sub-membrane cytoskeletal cortex of live eukaryotic cells was achieved for the first time, with high lateral resolution and a maximal time resolution of 8.5 s per frame (Fig. 2c). The cell cortex is a ubiquitous structure that lines the cytoplasmic face of the plasma membrane in eukaryotic cells [53]. It was discovered as a micron thick contractile gel present in amoeba and leukocytes, and upon purification, it was found to be rich in actin [54]. Actin binding proteins and molecular motors (myosins) were identified as being responsible for the passive and active mechanical properties of the actin cortex, namely. More recently, mechanical characterizations (many using atomic force microscopy), identified the actin cortex as the prime determinant of cell mechanics [53]. Interestingly, progresses in fluorescence and electron microscopy imaging showed that the actin cortex also plays a crucial role in plethora of important biological processes including mitosis, meiosis, cell–cell junctions [53], and in membrane protein diffusion restriction [55]. As those results established a fundamental interplay between cell mechanics and biological function, it became more and more important to understand the workings of the actin cortex at the molecular level. Unfortunately optical or electron microscopies lack either the spatial or temporal resolution to allow significant progress in our understanding of the actin cortex dynamics in live cells, and as a result the most insightful studies of the cortex were so far restricted to fixed cells. Eghiaian et al. used AFM in PeakForce mode to produce high-resolution snapshots of the cortex in live 3T3 fibroblasts at physiological temperature and in cell culture medium [51]. PeakForce tapping enables the simultaneous acquisition of a topographic and mechanical map of the sample, as a short force curve is performed at each pixel. Thanks to this wealth of information, the structural, mechanical and dynamical heterogeneity of the cortex at the subcellular level was uncovered. Two extreme cortex types co-existed, one being made out of large and thick actin bundles undergoing slow motion, and the second being made of an intricate meshwork of short filaments with apparent random orientation and high dynamics. On the basis of PeakForce mechanical maps, mechanical heterogeneity arising from the difference in connectivity between the densely connected 'mesh' and the more sparsely connected 'fibers' types of cortex were documented. Even though the maximum rate of that experiment (8.5 s per frame) did not enable studying the fastest actin rearrangements, HS-AFM at an acquisition rate of 1 Hz should enable to clearly decipher the molecular nature of events leading to actin cortical motion in the near future.

2.2. High-speed force spectroscopy (HS-FS): when experiment meets simulation

Before the development of forced single molecule protein unfolding, thermal and chemical protein unfolding were

thoroughly studied matters. Although only average ensemble techniques such as absorption, fluorescence, NMR spectroscopy and differential scanning calorimetry were available, many general concepts were then proposed that are still central to our knowledge of protein conformational dynamics [56–58]: The folding of proteins into their structure of lowest free energy is driven by the minimization of water exposure of hydrophobic residues, and the final structure is encoded in the protein sequence. To unfold a protein, overcoming an energy barrier is therefore necessary, which may be achieved by raising temperature, using chaotropic agents or by mechanically stretching the polypeptide chain. In 1997, Rief et al. took on a pioneering study of the mechanical stretching of titin, a protein that is responsible for the passive elasticity of striated muscles [19]. Titin is composed of Fn, PEVK, and immunoglobulin-like (Ig-like) domains. The ability of those Ig-like domains to unfold-refold upon stretching-relaxation of the muscle was thought to condition the physiological role of titin. In their groundbreaking work Rief et al. picked up titin adsorbed on gold with an AFM tip and pulled on it with velocities ranging from 0.01 to 3 μm/s measuring forces between 100 and 200 pN. Upon extension of titin, force-extension curves revealed a sawtooth pattern with peaks separated by ~25 nm, the stretched polypeptide length of an Ig-domain. Thus, each event in the force-*vs*-extension curve was interpreted to originate from the mechanical unfolding of a single Ig-like domain. The authors showed that the extension behavior of each unfolded domain was well explained by the worm-like chain model [59,60]. The unfolding forces were not of a constant value, but were spread, and depended on the pulling velocity. This behavior was predicted by the Bell-Evans model [61,62], which described the exponential modulation of the unfolding rate α (actually, this was an unbinding rate, since Bell was originally interested in cell adhesion) was exponentially modulated by force:

$$\alpha \approx \alpha_0 \cdot e^{\left(\frac{Fx}{k_B T}\right)} \qquad \text{and} \qquad \alpha_0 = A \cdot \left(\frac{E_a}{k_B T}\right)$$

where α is the unfolding rate under force, α_0 the unfolding rate in absence of force (following Arrhenius' law), A the Arrhenius' pre-exponential factor, F the mechanical force, x the width of the unfolding potential, E_a the unfolding activation energy, k_B Boltzmann's constant, and T the temperature. Finally, unfolded Ig-like domains of titin were able to refold when tension was released. This experiment was refined using polyproteins of the same titin domain, revealing an intermediate unfolding state documented by a 'hump' preceding complete Ig domain unfolding [63]. From molecular dynamics simulations and site-directed mutagenesis, the intermediate unfolding state was identified as the separation of two short β-strands. However, molecular dynamics simulations were not able to fully account for experimental observations, as pulling velocities *in silico* are about 3 orders of magnitude faster than that of AFM experiments. Besides, whereas some proteins are known to autonomously fold in μs timescales, conventional force spectroscopy at its maximal velocity triggered unfolding events in milliseconds, hence moving unfolding experiments to the μs time range had a significant interest.

To overcome this problem, Rico et al. adapted HS-AFM to perform high-speed force spectroscopy (HS-FS) to unfold titin I91 concatemers (polyproteins of 8 domains) over a range of velocities spanning 6 orders of magnitudes (from 0.0097 to 3870 μm/s), encompassing the range of molecular dynamics simulations (>2800 μm/s) [64] (Fig. 3a). At low speed, the unfolding forces matched previous reports and were well described by the Bell–Evans model. However graphing the unfolding force *vs* log(velocity) displayed a notable upturn at pulling velocities >100 μm/s (Fig. 3b). This deviation from the Bell–Evans model is accounted for by Hummer and Szabo's numerical model [65]: At low velocity, the protein has time to explore its conformational landscape during unfolding and thermal fluctuations are important. As the pulling velocity increases, this opportunity is not given to the protein and the unfolding force is mainly determined by the initial position of the protein within the energy landscape. In addition, the distance between the native and transition states varies as force is applied, leading to the non-linearity in the unfolding force *vs* log(velocity) plot. Importantly, the unfolding forces measured by HS-FS in the mm/s velocity range agreed in magnitude to those "measured" by molecular dynamics simulations [64]. Importantly, Hummer and Szabo's numerical model predicted a distance to the transition state of 0.89 nm, much larger than that reported from conventional AFM measurements ~0.3 nm [19,63], but similar to the distance at which the secondary structure of titin I91 breaks down in steered MD simulations [66]. Moreover, detailed analysis of the "hump" in the force traces provided novel insights into the mechanism of the intermediate unfolding state of titin I91. In the slow pulling regime, a constant unfolding force was observed for a wide range of loading rates, as reported before [67]. However, when velocity was increased using HS-FS, the unfolding force from the native to the intermediate state increased with the log(velocity), recovering the Bell–Evans behavior. This suggests that the

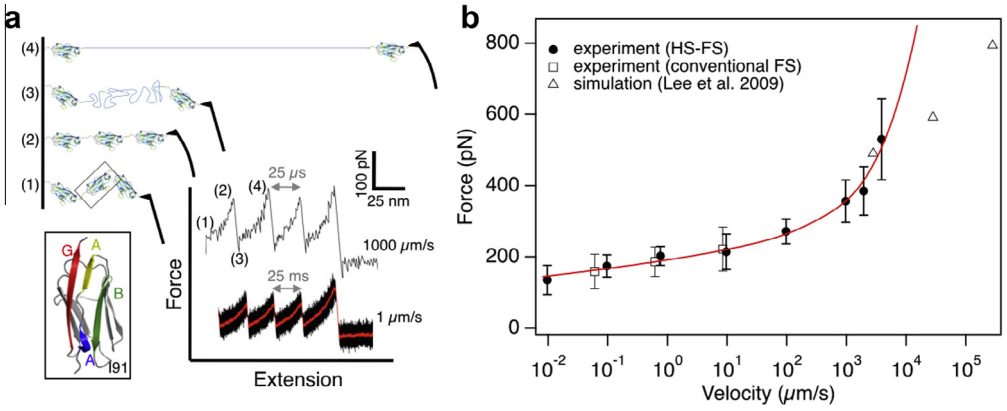

Fig. 3. High-speed force spectroscopy (HS-FS) of titin unfolding. (a) Schematic process of titin forced unfolding showing the relevant steps: (1) relaxed polyprotein, (2) polyprotein stretching, (3) unfolding of one domain and (4) unfolded domain stretching. Two examples of force extension curves revealing three unfolding peaks at 1 μm/s (bottom) and 1000 μm/s (top) are also shown. Gray arrows represent the time required to unfold and stretch a single domain. The inset shows the crystal structure of I91 domain with the relevant ß-strands in color (PDB 1TIT). (b) Dynamic force spectrum of titin I91 unfolding using HS-FS (●), conventional AFM (□) and MD simulations (△). Red line is the fit to the Hummer and Szabo model with a distance to the transition state of ~0.89 nm, an energy barrier of 36 k_BT and an intrinsic dissociation rate of $\sim 2 \times 10^{-10}$ s^{-1} [65].

two β-strands are in dynamic equilibrium between folded and unfolded states at physiologically relevant rates and forces. The fast time resolution of HS-FS of ~1 μs allowed the direct observation of this dynamic hopping between intermediate and native states.

3. Conclusions and outlook

In spite of being now more than a decade old, HS-AFM is only at the dawn of its possibilities for biological imaging. It is, to our knowledge, the only 'nanometer-resolution' technique that can self-sufficiently perform sub-second imaging of biological samples over long temporal stretches and manipulate the same sample to yield mechanical information on it. The development of wide-range scanners and combination with optical microscopy has endowed HS-AFM with the capacity to image cells and viruses giving it all the necessary power for state-of-the-art cellular biophysics. Altogether these developments allow dynamic imaging of membrane proteins at nanometer resolution in their membrane environment, and now even at the surface of bacteria or eukaryotic cells. This will soon lead to detailed structural–functional characterizations, for example to optically detect signal transduction events occurring as a consequence of plasma membrane remodeling. Meanwhile, the potential of HS-FS has not been fully exploited, since, to our knowledge, attempts to perform HS-FS for elasticity or receptor–ligand binding experiments have yet to be reported. Alternative to classical force spectroscopy approaches, multifrequency AFM consists in oscillating the AFM cantilever at multiple frequencies. This provides extra information on the tip-sample interaction and allows extracting mechanical properties of the sample, without impeding image acquisition [68]. Furthermore, the approach could allow excitation of the cantilever at a frequency higher than its first resonance and therefore permit faster scanning if the feedback is operated on this higher frequency.

Such developments could have a broad impact in the present era of cellular biophysics, as many cellular events might depend on mechano-transduction. We envision a distant future in which HS-AFM will have the power to detect single molecules at the cell surface and stimulate them with force, optical microscopy enabling to monitor the functional consequences of that stimulation at the intra-cellular level, yielding a much broader understanding of how cells transmit information from the membrane to the genes.

For now AFM and HS-AFM remain demanding techniques that require skill, knowledge and experience on the instruments as well as deep understanding of the physical-chemistry and/or biology of the sample. Here, we reviewed that HS-AFM and HS-FS methods just emerged for biological sample investigations able to provide researchers with so far inaccessible information. For example, the assessment of in-membrane plane interaction energies between membrane complexes, could not be assessed so far experimentally [30]. However, a series of elementary developments that simplify the machine, set standards and render data acquisition much more reproducible, are necessary conditions for broader acceptance among biologists. Nevertheless, in view of the excitement that HS-AFM imaging recently provoked in biophysics, we believe that it will take only little time before this versatile method can bring the full extent of its performance to biology, opening new fields of discovery in basic and applied biological research.

Acknowledgments

This work was supported by the Agence National de la Recherche (ANR) Grants Labex INFORM (ANR-11-LABX-0054) of the A*MIDEX program (ANR-11-IDEX-0001-02), grants (ANR-12-BS10-009-01 and ANR-12-BSV8-0006-01) and a European Research Council (ERC) Starting Grant (#310080).

References

[1] Binnig, G., Quate, C.F. and Gerber, C. (1986) Atomic force microscope. Phys. Rev. Lett. 56, 930.
[2] Meyer, G. and Amer, N.M. (1988) Novel optical approach to atomic force microscopy. Appl. Phys. Lett. 53, 1045–1047.
[3] Albrecht, T.R. and Quate, C.F. (1987) Atomic resolution imaging of a nonconductor by atomic force microscopy. J. Appl. Phys. 62.
[4] Binnig, G., Gerber, C., Stoll, E., Albrecht, T.R. and Quate, C.F. (1987) Atomic resolution with atomic force microscope. Europhys. Lett. 3.
[5] Giessibl, F. (2005) AFMs path to atomic resolution. Mater. Today 8, 32–41.
[6] Drake, B., Prater, C.B., Weisenhorn, A.L., Gould, S.A.C., Albrecht, T.R., Quate, C.F., Cannell, D.S., Hansma, H.G. and Hansma, P.K. (1989) Imaging crystals, polymers, and processes in water with the atomic force microscope. Science 243, 1586–1588.
[7] Fotiadis, D., Hasler, L., Muller, D.J., Stahlberg, H., Kistler, J. and Engel, A. (2000) Surface tongue-and-groove contours on lens MIP facilitate cell-to-cell adherence. J. Mol. Biol. 300, 779–789.
[8] Fotiadis, D., Liang, Y., Filipek, S., Saperstein, D.A., Engel, A. and Palczewski, K. (2003) Atomic-force microscopy: rhodopsin dimers in native disc membranes. Nature 421, 127–128.
[9] Muller, D.J., Hand, G.M., Engel, A. and Sosinsky, G.E. (2002) Conformational changes in surface structures of isolated connexin 26 gap junctions. EMBO J. 21, 3598–3607.
[10] Muller, D.J., Schabert, F.A., Buldt, G. and Engel, A. (1995) Imaging purple membranes in aqueous solutions at sub-nanometer resolution by atomic force microscopy. Biophys. J. 68, 1681–1686.
[11] Scheuring, S., Reiss-Husson, F., Engel, A., Rigaud, J.L. and Ranck, J.L. (2001) High-resolution AFM topographs of Rubrivivax gelatinosus light-harvesting complex LH2. EMBO J. 20, 3029–3035.
[12] Scheuring, S., Ringler, P., Borgnia, M., Stahlberg, H., Muller, D.J., Agre, P. and Engel, A. (1999) High resolution AFM topographs of the Escherichia coli water channel aquaporin Z. EMBO J. 18, 4981–4987.
[13] Scheuring, S. and Sturgis, J.N. (2005) Chromatic adaptation of photosynthetic membranes. Science 309, 484–487.
[14] Radmacher, M., Tillamnn, R.W., Fritz, M. and Gaub, H.E. (1992) From molecules to cells: imaging soft samples with the atomic force microscope. Science 257, 1900–1905.
[15] Radmacher, M., Tillmann, R.W. and Gaub, H.E. (1993) Imaging viscoelasticity by force modulation with the atomic force microscope. Biophys. J. 64, 735–742.
[16] Florin, E.L., Moy, V.T. and Gaub, H.E. (1994) Adhesion forces between individual ligand–receptor pairs. Science 264, 415–417.
[17] Lee, G.U., Chrisey, L.A. and Colton, R.J. (1994) Direct measurement of the forces between complementary strands of DNA. Science 266, 771–773.
[18] Moy, V.T., Florin, E.L. and Gaub, H.E. (1994) Intermolecular forces and energies between ligands and receptors. Science 266, 257–259.
[19] Rief, M., Gautel, M., Oesterhelt, F., Fernandez, J.M. and Gaub, H.E. (1997) Reversible unfolding of individual titin immunoglobulin domains by AFM. Science 276, 1109–1112.
[20] Cleveland, J.P., Manne, S., Bocek, D. and Hansma, P.K. (1993) A nondestructive method for determining the spring constant of cantilevers for scanning force microscopy. Rev. Sci. Instrum. 64.
[21] Ando, T., Kodera, N., Takai, E., Maruyama, D., Saito, K. and Toda, A. (2001) A high-speed atomic force microscope for studying biological macromolecules. Proc. Natl. Acad. Sci. 98, 12468–12472.
[22] Viani, M.B., Pietrasanta, L.I., Thompson, J.B., Chand, A., Gebeshuber, I.C., Kindt, J.H., Richter, M., Hansma, H.G. and Hansma, P.K. (2000) Probing protein–protein interactions in real time. Nat. Struct. Biol. 7, 644–647.
[23] Ando, T., Kodera, N., Takai, E., Maruyama, D., Saito, K. and Toda, A. (2001) A high-speed atomic force microscope for studying biological macromolecules. Proc. Natl. Acad. Sci. USA 98, 12468–12472.
[24] Kodera, N., Sakashita, M. and Ando, T. (2006) Dynamic proportional-integral-differential controller for high-speed atomic force microscopy. Rev. Sci. Instrum. 77.
[25] Kodera, N., Yamashita, H. and Ando, T. (2005) Active damping of the scanner for high-speed atomic force microscopy. Rev. Sci. Instrum. 76.
[26] Ando, T., Uchihashi, T. and Scheuring, S. (2014) Filming biomolecular processes by high-speed atomic force microscopy. Chem. Rev. 114, 3120–3188.
[27] Kodera, N., Yamamoto, D., Ishikawa, R. and Ando, T. (2010) Video imaging of walking myosin V by high-speed atomic force microscopy. Nature 468, 72–76.
[28] Kodera, N., Yamamoto, D., Ishikawa, R. and Ando, T. (2010) Video imaging of walking myosin V by high-speed atomic force microscopy. Nature 468, 72–76.
[29] Igarashi, K., Uchihashi, T., Koivula, A., Wada, M., Kimura, S., Okamoto, T., Penttilä, M., Ando, T. and Samejima, M. (2011) Traffic jams reduce hydrolytic efficiency of cellulase on cellulose surface. Science 333, 1279–1282.
[30] Casuso, I., Sens, P., Rico, F. and Scheuring, S. (2010) Experimental evidence for membrane-mediated protein–protein interaction. Biophys. J . 99, L47–L49.
[31] Casuso, I., Khao, J., Chami, M., Paul-Gilloteaux, P., Husain, M., Duneau, J.-P., Stahlberg, H., Sturgis, J.N. and Scheuring, S. (2012) Characterization of the

motion of membrane proteins using high-speed atomic force microscopy. Nat. Nanotechnol. 7, 525–529.
[32] Colom, A., Casuso, I., Boudier, T. and Scheuring, S. (2012) High-speed atomic force microscopy: cooperative adhesion and dynamic equilibrium of junctional microdomain membrane proteins. J. Mol. Biol. 423, 249–256.
[33] Milhiet, P.E., Yamamoto, D., Berthoumieu, O., Dosset, P., Le Grimellec, C., Verdier, J.M., Marchal, S. and Ando, T. (2010) Deciphering the structure, growth and assembly of amyloid-like fibrils using high-speed atomic force microscopy. PLoS ONE 5, e13240.
[34] Uchihashi, T., Iino, R., Ando, T. and Noji, H. (2011) High-speed atomic force microscopy reveals rotary catalysis of rotorless F1-ATPase. Science 333, 755–758.
[35] Kendrew, J.C., Dickerson, R.E., Strandberg, B.E., Hart, R.G., Davies, D.R., Phillips, D.C. and Shore, V.C. (1960) Structure of myoglobin: a three-dimensional fourier synthesis at 2 [angst], Resolution. Nature 185, 422–427.
[36] Deisenhofer, J., Epp, O., Miki, K., Huber, R. and Michel, H. (1985) Structure of the protein subunits in the photosynthetic reaction centre of *Rhodopseudomonas viridis* at 3Å resolution. Nature 318, 618–624.
[37] White, S. (2014) Membrane proteins of known 3D structure in.
[38] Berman, H.M., Westbrook, J., Feng, Z., Gilliland, G., Bhat, T.N., Weissig, H., Shindyalov, I.N. and Bourne, P.E. (2000) The protein data bank. Nucleic Acids Res. 28, 235–242.
[39] Wallin, E. and von Heijne, G. (1998) Genome-wide analysis of integral membrane proteins from eubacterial, archaean, and eukaryotic organisms. Protein Sci. 7, 1029–1038.
[40] Henderson, R. and Unwin, P.N. (1975) Three-dimensional model of purple membrane obtained by electron microscopy. Nature 257, 28–32.
[41] Yamashita, H., Voitchovsky, K., Uchihashi, T., Contera, S.A., Ryan, J.F. and Ando, T. (2009) Dynamics of bacteriorhodopsin 2D crystal observed by high-speed atomic force microscopy. J. Struct. Biol. 167, 153–158.
[42] Oesterhelt, D. and Stoeckenius, W. (1973) Functions of a new photoreceptor membrane. Proc. Natl. Acad. Sci. USA 70, 2853–2857.
[43] Haupts, U., Tittor, J. and Oesterhelt, D. (1999) Closing in on bacteriorhodopsin: progress in understanding the molecule. Annu. Rev. Biophys. Biomol. Struct. 28, 367–399.
[44] Neutze, R., Pebay-Peyroula, E., Edman, K., Royant, A., Navarro, J. and Landau, E.M. (2002) Bacteriorhodopsin: a high-resolution structural view of vectorial proton transport. Biochim. Biophys. Acta 1565, 144–167.
[45] Shibata, M., Yamashita, H., Uchihashi, T., Kandori, H. and Ando, T. (2010) High-speed atomic force microscopy shows dynamic molecular processes in photoactivated bacteriorhodopsin. Nat. Nanotechnol. 5, 208–212.
[46] Buzhynskyy, N., Hite, R.K., Walz, T. and Scheuring, S. (2007) The supramolecular architecture of junctional microdomains in native lens membranes. EMBO Rep. 8, 51–55.
[47] Yamashita, H., Voïtchovsky, K., Uchihashi, T., Contera, S.A., Ryan, J.F. and Ando, T. (2009) Dynamics of bacteriorhodopsin 2D crystal observed by high-speed atomic force microscopy. J. Struct. Biol. 167, 153–158.
[48] Colom, A., Casuso, I., Rico, F. and Scheuring, S. (2013) A hybrid high-speed atomic force–optical microscope for visualizing single membrane proteins on eukaryotic cells. Nat. Commun. 4.
[49] Fukuda, S., Uchihashi, T., Iino, R., Okazaki, Y., Yoshida, M., Igarashi, K. and Ando, T. (2013) High-speed atomic force microscope combined with single-molecule fluorescence microscope. Rev. Sci. Instrum. 84, 073706.
[50] Watanabe, H., Uchihashi, T., Kobashi, T., Shibata, M., Nishiyama, J., Yasuda, R. and Ando, T. (2013) Wide-area scanner for high-speed atomic force microscopy. Rev. Sci. Instrum. 84, 053702.
[51] Eghiaian, F., Rigato, A. F., Scheuring, S. (2014) Structural, mechanical, and dynamical variability of the cytoskeletal cortex in live cells, submitted.
[52] Rico, F., Su, C. and Scheuring, S. (2011) Mechanical mapping of single membrane proteins at submolecular resolution. Nano Lett. 11, 3983–3986.
[53] Salbreux, G., Charras, G. and Paluch, E. (2012) Actin cortex mechanics and cellular morphogenesis. Trends Cell Biol. 22, 536–545.
[54] Bray, D., Heath, J. and Moss, D. (1986) The membrane-associated 'cortex' of animal cells: its structure and mechanical properties. J. Cell Sci. Suppl. 4, 71–88.
[55] Kusumi, A., Suzuki, K.G., Kasai, R.S., Ritchie, K. and Fujiwara, T.K. (2011) Hierarchical mesoscale domain organization of the plasma membrane. Trends Biochem. Sci. 36, 604–615.
[56] Fersht, A.R. (1993) The sixth Datta Lecture. Protein folding and stability: the pathway of folding of barnase. FEBS Lett. 325, 5–16.
[57] Fersht, A.R. (1994) Jubilee Lecture. Pathway and stability of protein folding. Biochem Soc Trans. 22, 267–273.
[58] Ptitsyn, O.B. (1995) How the molten globule became. Trends Biochem. Sci. 20, 376–379.
[59] Marko, J.F. and Siggia, E.D. (1995) Statistical mechanics of supercoiled DNA. Phys. Rev. E Stat. Phys. Plasmas. Fluids Relat. Interdiscip. Top. 52, 2912–2938.
[60] Bustamante, C., Marko, J.F., Siggia, E.D. and Smith, S. (1994) Entropic elasticity of lambda-phage DNA. Science 265, 1599–1600.
[61] Evans, E. and Ritchie, K. (1997) Dynamic strength of molecular adhesion bonds. Biophys. J. 72, 1541–1555.
[62] Bell, G.I. (1978) Models for the specific adhesion of cells to cells. Science 200, 618–627.
[63] Marszalek, P.E., Lu, H., Li, H., Carrion-Vazquez, M., Oberhauser, A.F., Schulten, K. and Fernandez, J.M. (1999) Mechanical unfolding intermediates in titin modules. Nature 402, 100–103.
[64] Lee, E.H., Hsin, J., Sotomayor, M., Comellas, G. and Schulten, K. (2009) Discovery through the computational microscope. Structure 17, 1295–1306.
[65] Hummer, G. and Szabo, A. (2003) Kinetics from nonequilibrium single-molecule pulling experiments. Biophys. J. 85, 5–15.
[66] Rotsch, C. and Radmacher, M. (2000) Drug-induced changes of cytoskeletal structure and mechanics in fibroblasts: an atomic force microscopy study. Biophys. J. 78, 520–535.
[67] Nunes, J.M., Hensen, U., Ge, L., Lipinsky, M., Helenius, J., Grubmuller, H. and Muller, D.J. (2010) A "force buffer" protecting immunoglobulin titin. Angew. Chem. Int. Ed. Engl. 49, 3528–3531.
[68] Garcia, R. and Herruzo, E.T. (2012) The emergence of multifrequency force microscopy. Nat. Nanotechnol. 7, 217–226.